

O. Toktarbaiuly^{1*}, A. Kurbanova¹, O. Ualibek¹, A. Seralin¹,
T. Zhunussova¹, G. Sugurbekova², N. Nuraje¹

¹National Laboratory Astana, Nazarbayev University, Nur-Sultan, Kazakhstan;

²LLP "EcoStandart.kz", Nur-Sultan, Kazakhstan

(*Corresponding author's e-mail: olzat.toktabaiuly@nu.edu.kz)

Fabrication of Superhydrophobic Self-Cleaning Coatings by Facile Method: Stable after Exposure to Low Temperatures and UV Light

Self-cleaning hydrophobic surfaces attracted public attention last few decades after discovering of lotus effect. Ability of lotus leaves to keep cleanness in relatively dirty places and to clean up itself during rains directed to the development of novel materials and surface structure modification. The surface with such smart properties may have the potential for cost-effectiveness in the case of application in skyscrapers, high buildings, etc. Two main criteria for the surface to express hydrophobic behavior are roughness and low surface energy of the coating material. In this study, superhydrophobic self-cleaning coatings were prepared by a simple, facile, and cheap method using easily available materials, such as polydimethylsiloxane (PDMS) and TiO₂ nanoparticles, and fully characterized for direct usage. PDMS is a bonding layer and TiO₂ nanoparticles are a reinforced composite to form roughness, which shows superhydrophobicity. Characterizations showed that the prepared superhydrophobic coating has a water contact angle of up to 165.5°, with sliding angle of less than 5°. Also self-cleaning and surface microfluidic properties have been studied. The superhydrophobic properties of these coatings do not change even after exposure to their surface to low temperatures and UV light. SEM images confirm the rough structure of obtained surface on glass and sand grains.

Keywords: superhydrophobic coating, superhydrophobic sand, polydimethylsiloxane, titanium oxide nanoparticles, contact angle, UV light, facile method, electrokinetic potential.

Introduction

Recently, the fabrication of superhydrophobic surfaces and coatings based on oxides and polymers with exceptional water repellency is a relevant topic. Superhydrophobic surfaces are essential for the energy-saving industry, because such surfaces are not limited to self-cleaning protection properties, but are also used for anti-icing applications [1]. The effect of roughness on the surface and energy of the fabricated substrate plays a key role in creating superhydrophobic properties and is used to prevent ice accumulation on the substrate [2, 3]. When a drop of water hits a solid surface, it tends to a lower energy state and is measured using the contact angle of water wetting (the radius of the three-phase contact line: solid-liquid-air) of each drop [1]. The hydrophobic surface is described as a surface in which the contact angle of water exceeds 110°, and a drop of water reluctantly slides off its surface [4].

At present, much attention is paid to the preparation of a hydrophobic surface, which is widely used as a self-cleaning coating [5], corrosion protection [6, 7], water-oil separation [8, 9], and anti-icing [10, 11]. Until now, many superhydrophobic coatings with proposed applications have been made with various methods, such as corrosion resistance [12–14], anti-fog surfaces [15–17], anti-icing surfaces [16–20], oil and water separation [21–24], self-cleaning surfaces [25–28], battery production technology [29], sensors [30, 31], water treatment [32], optical devices [33], etc.

Experimental

Chemicals

High purity titanium (IV) oxide nanoparticles (TiO₂, 99.5 %, size 21 nm), PDMS (Silicone Sealant), anhydrous hexane (95 %), borosilicate cover glasses were purchased from Sigma Aldrich. Mixed carbonate-silicate sand from the Akmola region of Kazakhstan with a grain size of 0.1 μm to 800 μm was used as raw material and quartz sand was purchased from LLP "Labopharma" with the GOST 9428-73.

Preparation of Superhydrophobic Solution

Firstly, 1 g PDMS was dissolved in 10 ml of hexane by magnetic stirring for 3 hours, then placed into an ultrasound bath for 1 h under a hermetically covered cap. Further, TiO₂ was added to the mixture and ultra-sonicated another 2 h.

Preparation of Superhydrophobic Coating on Glass by Coating with Sliding Scraper

The glass substrate was repeatedly cleaned several times with deionized water and ethanol, then dried in an oven at 60 °C. The as-prepared superhydrophobic solution was coated by a sliding scraper onto the surface of the glass substrate. Further, the glass substrate was placed in the driving oven at 70 °C for 30 min and annealed at 300 °C for 10 min. Figure 1 shows a complete schematic picture of the experimental synthesis of superhydrophobic coatings.

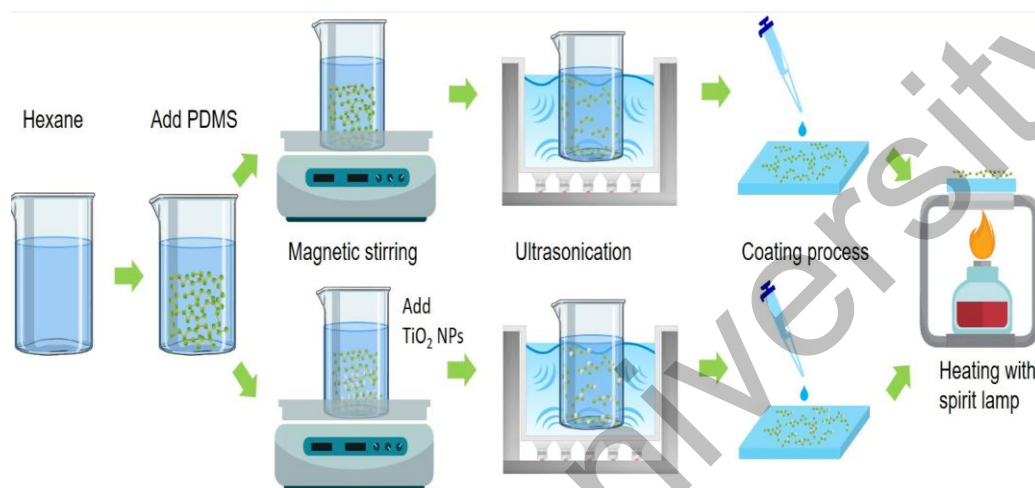


Figure 1. Schematic of a process for synthesis of a superhydrophobic solution and coating

Preparation of Superhydrophobic Sands

Carbonate-silicate sand from the Akmola region of Kazakhstan and quartz sand were used experimentally to make superhydrophobic sands. Akmola sand was cleaned with deionized water in an ultrasonic bath for 30 minutes. The cleaned sand was dried at 70 °C for 30 minutes. The synthesized superhydrophobic suspensions were applied to sand in the same manner as described above.

Characterization

The surface of the materials was studied by Scanning Electron Microscope (SEM) using a Zeiss Auriga Crossbeam 540. The zeta potential and size distribution of suspension were measured by a Zetasizer 3000 (Malvern Instruments). The static contact angle of the droplets was measured by a contact angle meter (OCA 15 EC, Neurtek Instruments). Zeta potential and size distribution were conducted three times. Also, all contact angle measurements were examined at least five times, the average value was taken. Standard deviation was calculated by following formulas:

$$STD = \sqrt{\frac{(x_1 - \bar{x})^2 + (x_2 - \bar{x})^2 + (x_3 - \bar{x})^2 + \dots}{n - 1}}; \quad (1)$$

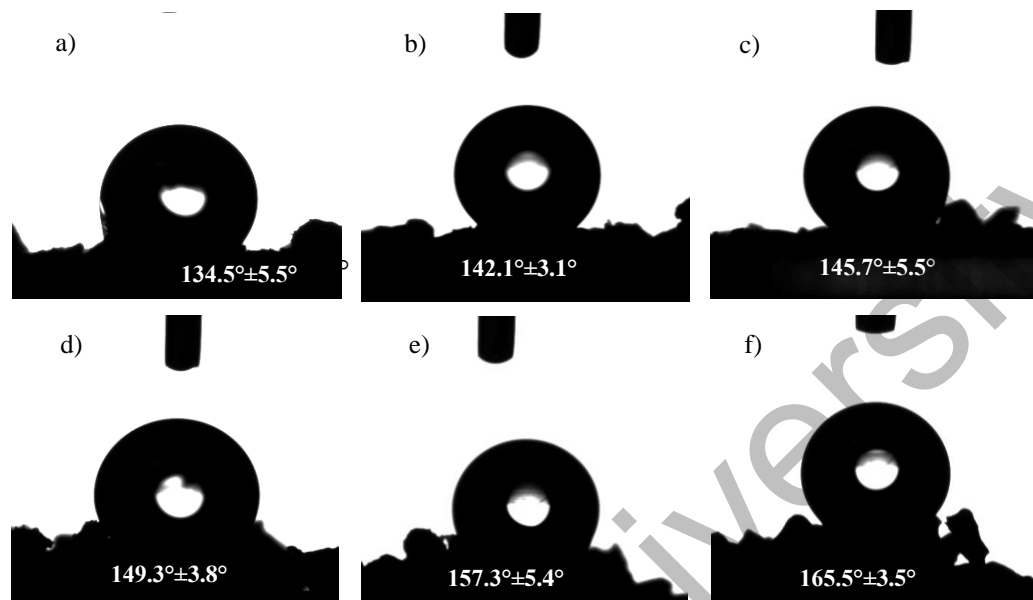
$$RSD = \frac{100}{\bar{x}}, \quad (2)$$

where \bar{x} — the average result; STD — the standard deviation; RSD — the relative standard deviation (%); n — the total number of observation.

Results and Discussion

Wettability of superhydrophobic sands was investigated with optical contact angle measuring and contour analysis system. To measure contact angle, sand particles were uniformly distributed on the surface of conductive double-sided carbon tape and thereafter placed in to sample stage. An amount of 10 μ l water droplet was applied to all samples. Figure 2 shows contact angle measurements of quartz sand, cleaned and not cleaned Akmola sand after processing with superhydrophobic coatings. Wettability of three different

sands (quartz sand, not cleaned, and cleaned Akmola sand) was analysed after coating PDMS and the results are shown in the top row of Figure 2. Water contact angles were $134.5^{\circ} \pm 5.5^{\circ}$, $142.1^{\circ} \pm 3.1^{\circ}$, and $145.7^{\circ} \pm 2.9^{\circ}$ for these sands, respectively. Furthermore, mixture of PDMS and TiO_2 nanoparticles (NPs) was coated on the surface of these sands. The bottom row of Figure 2 represents the contact angle analysis and superhydrophobic properties of these sands can be seen from the results. Water contact angles were $149.3^{\circ} \pm 3.8^{\circ}$, $157.3^{\circ} \pm 5.4^{\circ}$, and $165.5^{\circ} \pm 3.5^{\circ}$ for these sands.



Top row: *a* — PDMS coated quartz sand; *b* — uncleaned Akmola sand; *c* — cleaned Akmola sand.
 Bottom row: *d* — mixture of PDMS and TiO_2 NPs coated quartz sand; *e* — uncleaned Akmola sand;
f — cleaned Akmola sand

Figure 2. Contact angle measurements of different sands before and after coating PDMS and PDMS/ TiO_2

Figure 3 demonstrates the comparison of TiO_2 NPs effects on hydrophobic properties of sand. An increase of contact angle can be seen after applying TiO_2 NPs with PDMS. This also indicates the useful impacts of TiO_2 on the process of superhydrophobic materials. The highest contact angle was achieved from cleaned Akmola sand after coating mixture of PDMS and TiO_2 NPs and it was $165.5^{\circ} \pm 3.5^{\circ}$. This result evidenced that cleaning procedure effectively improves superhydrophobic properties of sand.

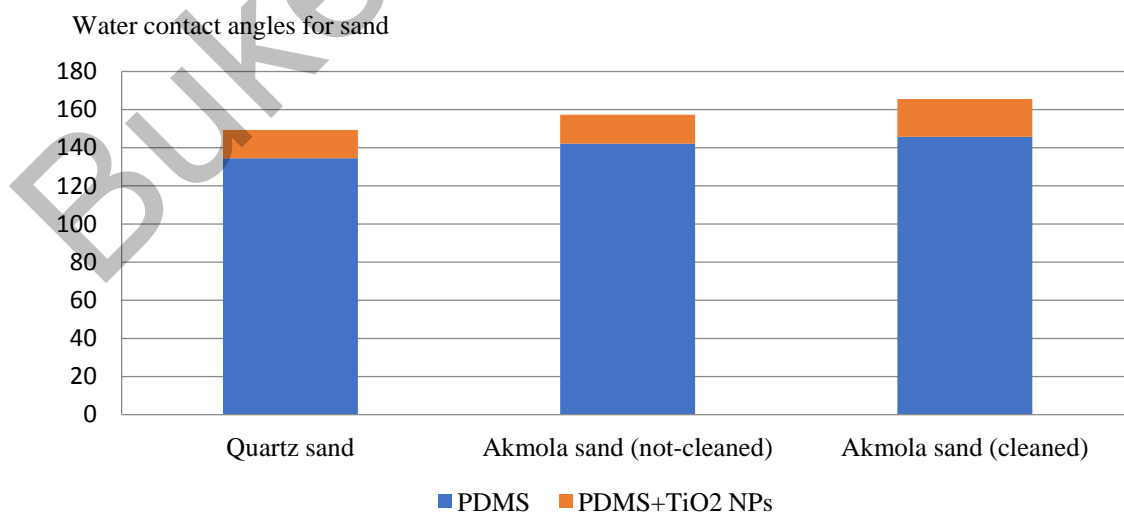
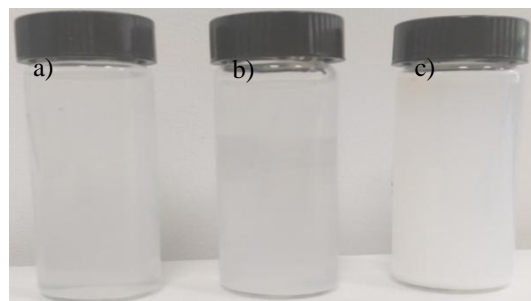


Figure 3. A diagram for water contact angle of obtained superhydrophobic sands

Inhomogeneous dispersion due to the pronounced tendency of nanoparticles to agglomerate is a common phenomenon in the synthesis of polymer nanocomposite. However, good dispersion is required to obtain nanocomposites with optimized properties. The dispersant has branched polysilicon chains that can bind to the -OH group on the TiO₂ surface. Figure 4 illustrates the dispersion of PDMS + TiO₂. A stable and homogenized dispersion indicates that the silicone polymer dissolved in hexane is bound to the surface of the TiO₂ particles.



a — TiO₂; b — PDMS; c — PDMS/TiO₂ in hexane

Figure 4. Visual comparison of solutions

The study results showed a rather large agglomeration with an average hydrodynamic diameter of 812.9 ± 3.6 nm and an average Pdi (polydispersity index) of 0.156 ± 0.003 , and the diameters of TiO₂, PDMS, PDMS/TiO₂ are equal at 501.5 ± 3.8 nm, 784.2 ± 4.2 nm, 1153.1 ± 2.7 nm, respectively (Table 1). Inhomogeneous dispersion due to the pronounced tendency of nanoparticles to agglomerate is a common phenomenon in the synthesis of polymer nanocomposite [34]. When titanium oxide was added to the silicone polymer, the particle size increased from ~ 500 nm to 1000 nm (Figure 5).

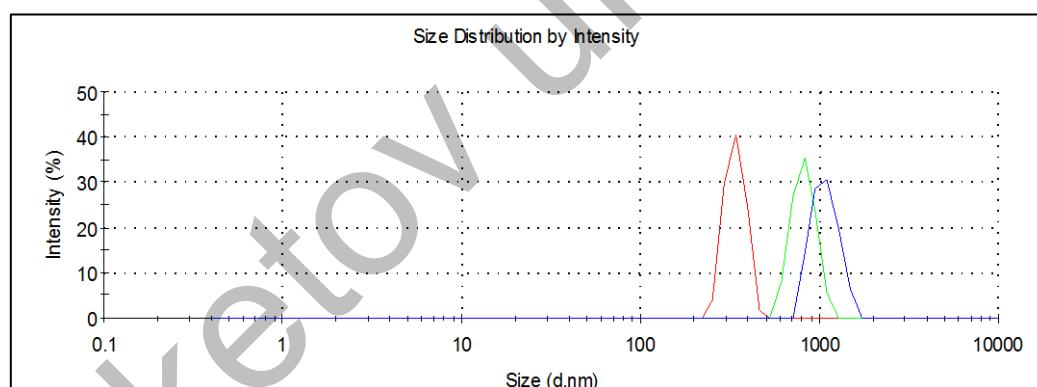


Figure 5. Zeta potential (ζ) of (red line) TiO₂, (green line) PDMS, (blue line) PDMS/TiO₂

The average electro kinetic (zeta " ζ ") dispersion potential was 0.0289 ± 0.02 mV and the average hydrodynamic diameter was 812.9 ± 3.6 nm (Table 1), indicating that some agglomerates and nanoparticles are present in the suspension.

Table 1

Stability of dispersion

Parameters	TiO ₂ in hexane	PDMS in hexane	PDMS/TiO ₂ in hexane	Average value
Size average (d, nm)	501.5 ± 3.8	784.2 ± 4.2	1153.1 ± 2.7	812.9 ± 3.6
PDI	0.163 ± 0.004	0.152 ± 0.002	0.155 ± 0.003	0.157 ± 0.003
ζ (mV)	0.0539 ± 0.02	0.0309 ± 0.04	0.00182 ± 0.002	0.0289 ± 0.02

The wettability of sand increased with the inflow due to an increase in the amount TiO₂, reaching a superhydrophobic effect with a contact angle of 165.5° at 6 mg of TiO₂, 157.3° at 5 mg of TiO₂. The increase in contact angle can be attributed to surface roughness due to the formation of a bonding of titanium parti-

cles. The contact angle of a sample was sharply decreased after 7 mg of TiO_2 , reaching 145.7° . Figure 6 demonstrates that all samples have a hydrophobic effect with a contact angle above 90° .

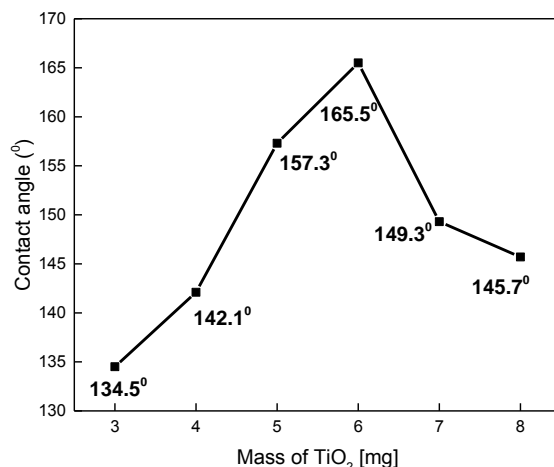


Figure 6. Dependence of contact angle on mass of TiO_2

The microstructure and surface morphology of various sands has been studied using SEM. Figure 7 shows SEM images of quartz sand before (a, b, c) and after coating PDMS (d, e, f) and PDMS/ TiO_2 (h, i, j) with different magnification. The images for micro area were confirmed effectively coating of superhydrophobic materials on the sand surface (see Figure 7 (c, f, g)). The microstructure of sand surface was changed and produced a rougher surface after applying PDMS and PDMS/ TiO_2 . The mixture of PDMS/ TiO_2 demonstrated a greater effect on superhydrophobicity. Moreover, cleaned and un-cleaned Akmol sands were imaged with SEM before and after processing with superhydrophobic materials. SEM images of cleaned (Figure 8) and uncleaned Akmol sand (Figure 9) before (a, b, c) and after coating PDMS (d, e, f), also PDMS/ TiO_2 (h, i, j) with different magnification. A smooth and uniform coating layer of superhydrophobic material can be seen in these images. Also, the effect of the cleaning process on the Akmol sand is clearly visible. Small dust and clay particles disappeared from the surface of sand after cleaning with water and difference can be seen in Figures 8 (b, c) and 9 (b, c). A clean surface provides better sticking of superhydrophobic material. For this reason, the highest contact angle was achieved from cleaned Akmol sand (the contact angle was increased from $157.3^\circ \pm 5.4^\circ$ to $165.5^\circ \pm 3.5^\circ$ after using cleaned Akmol sand).

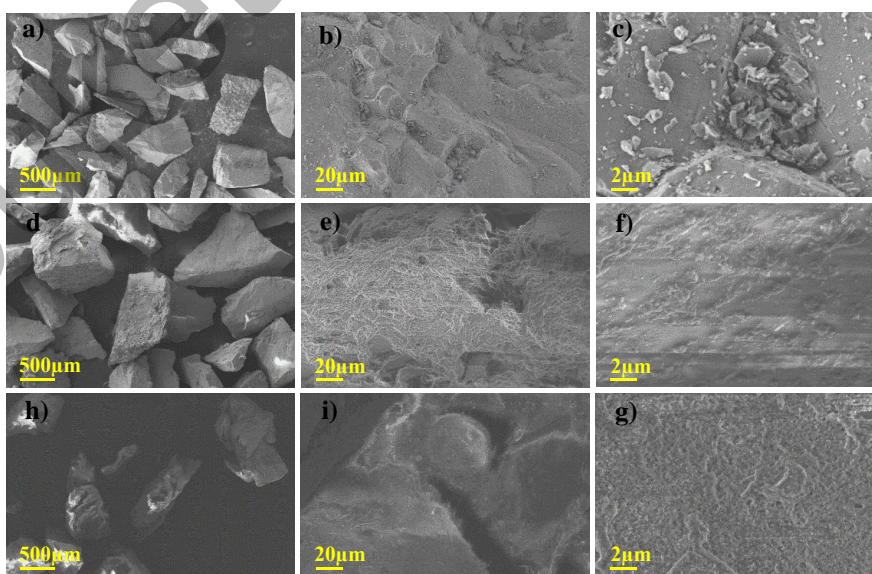


Figure 7. SEM images of quartz sand before (a, b, c) and after coating PDMS (d, e, f), also PDMS/ TiO_2 (h, i, j) with different magnification

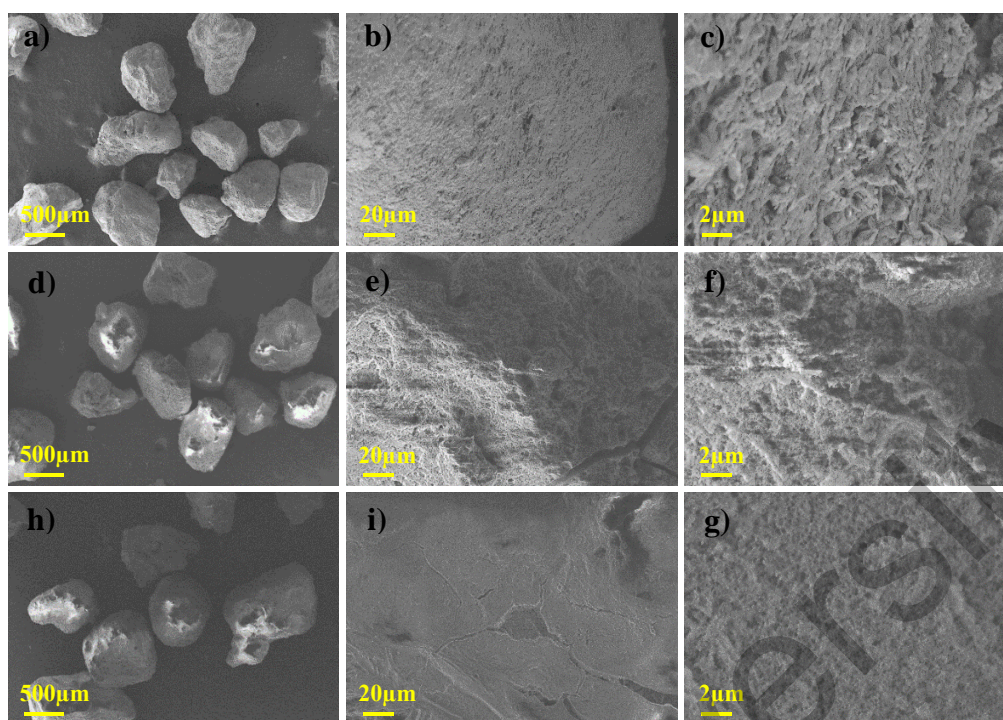


Figure 8. SEM images of uncleaned Akmol sand before (*a, b, c*) and after coating PDMS (*d, e, f*), also PDMS/TiO₂ (*h, i, j*) with different magnification

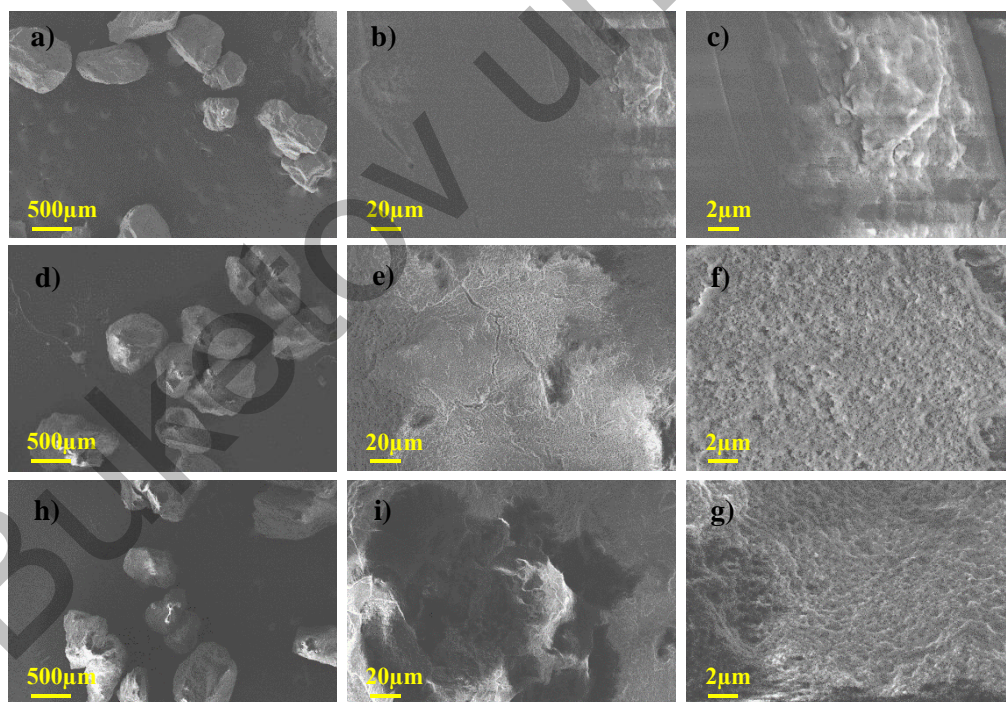


Figure 9. SEM images of cleaned Akmol sand before (*a, b, c*) and after coating PDMS (*d, e, f*), also PDMS/TiO₂ (*h, i, j*) with different magnification

Microfluidics was studied on the surfaces of superhydrophobic sand (Figure 10). The fluidity of water with blue dye on these surfaces is high with an inclination angle of 45°. These surfaces have a high self-cleaning ability because any dust or contamination can be easily removed with the water droplets at this inclination angle of 45° (Figure 11).



Figure 10. The microfluidity of water with blue dye on surfaces of superhydrophobic sands of quartz and Akmola region



Figure 11. Self-cleaning properties of superhydrophobic surfaces of quartz and Akmola region sand

The PDMS/TiO₂ coatings of quartz and uncleaned Akmola sand were placed in the lab refrigerator at low temperatures (−20 °C, −50 °C) for 72 hours. UV light (400 W) was exposed to these surfaces at room temperature for 24 hours to study the stability of their superhydrophobic properties. After exposure to low temperatures, these surfaces were warmed up to room temperatures to study contact angle properties. As seen in Figure 12, contact angle measurement demonstrates that both sands with coatings are still stable after low temperature and UV light exposure. This type of experiment was done three times to make sure that superhydrophobic properties do not change after a few cycles of temperature variety.

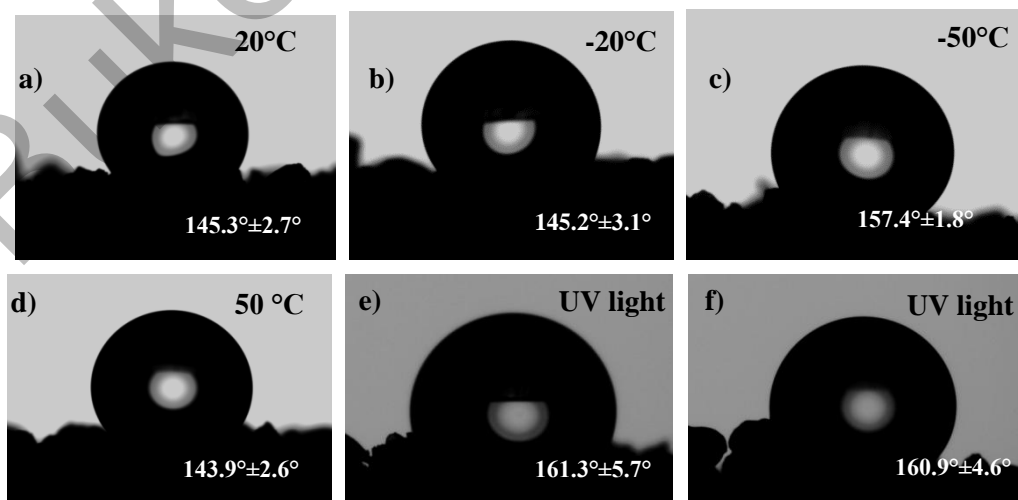


Figure 12. Contact angle measurements of quartz and uncleaned Akmola region sand with PDMS/TiO₂ coatings after exposure to low temperatures and UV light

Conclusions

Superhydrophobic self-cleaning coatings based on PDMS and PDMS/TiO₂ were synthesized using a facile chemical method. These superhydrophobic composites were applied to two different sands (quartz and sand from the Akmol region). The highest contact angle of water wetting of 165.5° was shown by the cleaned Akmol sand coated with PDMS/TiO₂, which has superhydrophobic properties.

The superhydrophobic properties of materials, such as wettability, particle size, and electrokinetic potential, were investigated. Also, these coatings demonstrated a microfluidity process on their surfaces, where the self-propelled flow is driven by the surface tension-induced pressure gradient. The superhydrophobic properties were retained after exposure to low temperatures and UV light.

These superhydrophobic self-cleaning materials by the facile method can be potentially used in construction to obtain concrete, anti-ice paving slabs, building facades, roofs, and waterproofing of buildings.

Acknowledgments

This research was funded by the Ministry of Education and Science of the Republic of Kazakhstan, grant AP08052848.

References

- 1 Si, Y., Dong, Z., & Jiang, L. (2018). Bioinspired Designs of Superhydrophobic and Superhydrophilic Materials. *ACS Central Science*, 4 (9), 1102–1112. <https://doi.org/10.1021/acscentsci.8b00504>
- 2 Ruan, M., Li, W., Wang, B., Deng, B., Ma, F., & Yu, Z. (2013). Preparation and Anti-icing Behavior of Superhydrophobic Surfaces on Aluminum Alloy Substrates. *Langmuir*, 29, 27, 8482–8491. <https://doi.org/10.1021/la400979d>
- 3 Wu, X., Silberschmidt, V.V., Hu, Z.-T., & Chen, Z. (2019). When superhydrophobic coatings are icephobic: Role of surface topology. *Surface & Coatings Technology*, 358: 207–214. <https://doi.org/10.1016/j.surfcoat.2018.11.039>
- 4 Tian, X., Verho, T., & Ras, R.H. (2016). SURFACE WEAR. Moving superhydrophobic surfaces toward real-world applications. *Science*. Apr 8; 352(6282):142–143. <https://doi.org/10.1126/science.aaf2073>
- 5 Zhou, X., Yu, S., Jiao, S., Lv, Z., Liu, E., Zhao, Y., & Cao, N. (2019). Fabrication of superhydrophobic TiO₂ quadrangular nanorod film with self-cleaning, anti-icing properties. *Ceram. Int*, 45, 11508–11516. <https://doi.org/10.1016/j.ceramint.2019.03.020>
- 6 Xue, Y., Wang, S., Zhao, G., Taleb, A., & Jin, Y. (2019). Fabrication of Ni-Co coating by electrochemical deposition with high super-hydrophobic properties for corrosion protection. *Surface Coating Technology*, 363, 352–361. <https://doi.org/10.1016/j.surfcoat.2019.02.056>
- 7 Liang, J., Wu, X.-W., Ling, Y., Yu, S., & Zhang, Z. (2018). Trilaminar structure hydrophobic graphene oxide decorated organosilane composite coatings for corrosion protection. *Surface Coating Technology*, 339, 65–77. <https://doi.org/10.1016/j.surfcoat.2018.02.002>
- 8 Yu, L., Zhang, Z., Tang, H., & Zhou, J. (2019). Fabrication of hydrophobic cellulosic materials via gas-solid silylation reaction for oil/water separation. *Cellulose*, 26, 4021–4037. <https://doi.org/10.1007/s10570-019-02355-7>
- 9 Sun, S., Zhu, L., Liu, X., Wu, L., Dai, K., Liu, C., Shen, C., Guo, X., Zheng, G., & Guo, Z. (2018). Superhydrophobic shish-kebab membrane with self-cleaning and oil/water separation properties. *ACS Sustainable Chem. Eng*, 6, 9866–9875. <https://doi.org/10.1021/acssuschemeng.8b01047>
- 10 Nguyen, T.-B., Park, S., & Lim, H. (2018). Effects of morphology parameters on anti-icing performance in superhydrophobic surfaces. *Applied Surface Science*, 435, 585–591. <https://doi.org/10.1016/j.apsusc.2017.11.137>
- 11 Qi, Y., Chen, S., & Zhang, J. (2019). Fluorine modification on titanium dioxide particles: Improving the anti-icing performance through a very hydrophobic surface. *Appl. Surf. Sci*, 476, 161–173. <https://doi.org/10.1016/j.apsusc.2019.01.073>
- 12 Barkhudarov, P.M., Shan, P.B., Watkins, E.B., Doshi, D.A., Brinker, C.J., & Majewski, J. (2008). Corrosion inhibition using superhydrophobic films. *Corrosion Science*, 50, 897–902. <https://doi.org/10.1016/j.corsci.2007.10.005>
- 13 Ishizaki, T., & Saito, N. (2010). Rapid formation of a superhydrophobic surface on a magnesium alloy coated with a cerium oxide film by a simple immersion process at room temperature and its chemical stability. *Langmuir*, 26, 9749–9755. <https://doi.org/10.1021/la100474x>
- 14 Zhang, F., Chen, S., Dong, L., Lei, Y., Liu, T., & Yin, Y. (2011). Preparation of superhydrophobic films on titanium as effective corrosion barriers. *Appl. Surf. Sci*, 257, 2587–2591. <https://doi.org/10.1016/j.apsusc.2010.10.027>
- 15 Dong, H., Ye, P., Zhong, M., Pietrasik, J., Drumright, R.E., & Matyjaszewski, K. (2010). Superhydrophilic surfaces via polymer–SiO₂ nanocomposites. *Langmuir*, 26, 15567–15573. <https://doi.org/10.1021/la102145s>
- 16 Lu, X., Wang, Z., Yang, X., Xu, X., Zhang, L., Zhao, N., & Xu, J. (2011). Antifogging and antireflective silica film and its application on solar modules. *Surface Coating Technology*, 206, 1490–1494. <https://doi.org/10.1016/j.surfcoat.2011.09.031>
- 17 You, J.-H., Lee, B.-I., Lee, J., Kim, H., & Byeon, S.-H. (2011). Superhydrophilic and antireflective La(OH)₃/SiO₂-nanorod/nanosphere films. *J. Coll. Interf. Sci*, 354, 373–379. <https://doi.org/10.1016/j.jcis.2010.10.009>

- 18 Jung, S., Tiwari, M.K., Doan, N.V., & Poulikakos, D. (2012). Mechanism of supercooled droplet freezing on surfaces. *Nat. Comm.*, 3, 615. <https://doi.org/10.1038/ncomms1630>
- 19 Tourkine, P., Le Merrer, M., & Quèrè, D. (2009). Delayed freezing on water repellent materials. *Langmuir*, 25, 7214–7216. <https://doi.org/10.1021/la900929u>
- 20 Meuler, A.J., Smith, J.D., Varanasi, K.K., Mabry, J.M., McKinley, G.H., & Cohen, R.E. (2010). Relationships between water wettability and ice adhesion. *ACS Appl. Mater. Interf.*, 2, 3100–3110. <https://doi.org/10.1021/am1006035>
- 21 Gui, X., Li, H., Wang, K., Wei, J., Jia, Y., Li, Z., Fan, L., Cao, A., Zhu, H., & Wu, D. (2011). Recyclable carbon nanotube sponges for oil absorption. *Acta Mater.*, 59, 4798–4804. <https://doi.org/10.1016/j.actamat.2011.04.022>
- 22 Pan, Q., Wang, M., & Wang, H. (2008). Separating small amount of water and hydrophobic solvents by novel superhydrophobic copper meshes. *Appl. Surf. Sci.*, 254, 6002–6006. <https://doi.org/10.1016/j.apsusc.2008.03.034>
- 23 Wang, C., Yao, T., Wu, J., Ma, C., Fan, Z., Wang, Z., Cheng, Y., Lin, Q., & Yang, B. (2009). Facile approach in fabricating superhydrophobic and superoleophilic surface for water and oil mixture separation. *ACS Appl. Mater. Interf.*, 1, 2613–2617. <https://doi.org/10.1021/am900520z>
- 24 Wen, Q., Di, J., Jiang, L., Yu, J., & Xu, R. (2013). Zeolite-coated mesh film for efficient oil–water separation. *Chem. Sci.*, 4, 591–595. <https://doi.org/10.3866/PKU.WHXB201906044>
- 25 Blossey, R. (2003). Self-cleaning surfaces — virtual realities. *Nature Mater.*, 2, 301–306.
- 26 Liu, K., & Jiang, L. (2011). Multifunctional integration: from biological to bio-inspired materials. *ACS Nano*, 5, 6786–6790. <https://doi.org/10.1021/nn203250y>
- 27 Parkin, I.P., & Palgrave, R.G. (2005). Self-cleaning coatings. *J. Mater. Chem.*, 15, 1689–1695.
- 28 Sanchez, C., Arribart, H., & Guille, M.M.G. (2005). Biomimetism and bioinspiration as tools for the design of innovative materials and systems. *Nat. Mater.*, 4, 277–288. <https://doi.org/10.1038/nmat1339>
- 29 Lifton, V.A., Simon, S., & Frahm, R.E. (2005). Reserve battery architecture based on superhydrophobic nanostructured surfaces. *Bell Labs Tech. J.*, 10, 81–85. <https://doi.org/10.1002/bltj.20105>
- 30 Andreeva, N., Ishizaki, T., Baroch, P., & Saito, N. (2012). High sensitive detection of volatile organic compounds using superhydrophobic quartz crystal microbalance. *Sens. Actuators B*, 164, 15–21. <https://doi.org/10.1016/j.snb.2012.01.051>
- 31 Cho, D.J., Kim, S.E., Seo, E., Lee, M.C., Lee, J.M., & Ko, J.S. (2013). Underwater micro gas detector. *Sens. Actuators B*, 188, 347–353.
- 32 Zhu, H., Chen, D., Li, N., Xu, Q., Li, H., He, J., & Lu, J. (2017). Dual-layer copper mesh for integrated oil-Water separation and water purification. *Appl. Catal. B*, 200, 594–600. <https://doi.org/10.1016/j.apcatb.2016.07.028>
- 33 Lin, C.-Y., Andrew Lin, K.-Y., Yang, T.-W., Chen, Y.-C., & Yang, H. (2017). Self-assembled hemispherical nanowell arrays for superhydrophobic antireflection coatings. *J. Colloid Interface Sci.*, 490, 174–180. <https://doi.org/10.1016/j.jcis.2016.11.064>
- 34 Carpi, F., Gallone, G., Galantini, F., & De Rossi, D. (2008). Silicone-Poly(hexylthiophene) blends as elastomers with enhanced electromechanical transduction properties. *Adv. Funct Mater.*, 18, 235–242. <https://doi.org/10.1002/adfm.200700757>

О. Тоқтарбайұлы, А. Курбанова, О. Уалибек, А. Сералин,
Т. Жунусова, Г. Сугурбекова, Н. Нурадже

Жеңіл әдіспен төмен температура мен ультракүлгін сәулесінің әсерінен кейін тұрақты супергидрофобты өзін-өзі тазартатын жабындарды дайындау

Өзін-өзі тазартатын гидрофобты беттер лотос эффектісі ашылғаннан кейін соңғы бірнеше онжылдықта қоғамның назарын өзіне аударды. Лотос гүлінің жапырақтарының салыстырмалы түрде лайлы жерлерде таза болып қалуы және жаңбыр кезінде өзін-өзі тазарту қабілеті жаңа материалдар мен бет құрылымының модификациясын дамытуға әкелді. Мұндай ақылды жабыны бар беттер көк тіреген ғимараттарда, зәулім ғимараттарда және т.б. пайдаланған кезде экономикалық әлеуетке ие болуы мүмкін. Беттің гидрофобты болуының екі негізгі критерийі — бұл беттің кедір-бұдырлығы және жабын материалының төмен беттік энергиясы. Осы зерттеуде супергидрофобты өзін-өзі тазартатын жабындар полидиметилсилоксан (ПДМС) және TiO_2 нанобөлшектері сияқты оңай қол жетімді материалдарды пайдалана отырып, қарапайым, жеңіл және арзан әдіспен дайындалды және тікелей пайдалану үшін толығымен сипатталған. ПДМС байланыстырушы қабат болып табылады, ал TiO_2 нанобөлшектері супергидрофобтылықты тудыратын кедір-бұдыр түзуге арналған армиленген композитке ие. Сипаттама жаңадан дайындалған супергидрофобты жабынның сумен жанасу бұрышы $165,5^\circ$ дейін, сырғанау бұрышы 5° -ден аз екенін көрсетті. Сонымен қатар өзін-өзі тазарту және беттік микрофлюидтік қасиеттері зерттелді. Бұл жабындардың супергидрофобты қасиеттері оның бетіне төмен температура мен ультракүлгін сәулесінің әсерінен кейін де өзгермейді. СЭМ суреттері шыны және құм түйіршіктерінде алынған беттің өрескел құрылымын растайды.

Кілт сөздер: супергидрофобты жабын, супергидрофобты құм, полидиметилсилоксан, титан оксидінің нанобөлшектері, шеттік бұрышы, УК-сәулелену, жеңіл әдіс, электрокинетикалық потенциал.

О. Токтарбайулы, А. Курбанова, О. Уалибек, А. Сералин,
Т. Жунусова, Г. Сугурбекова, Н. Нурадже

Получение супергидрофобных самоочищающихся покрытий легким методом: устойчивых к воздействию низких температур и ультрафиолетового излучения

За последние несколько десятков лет самоочищающиеся гидрофобные поверхности привлекли обширное внимание после открытия эффекта лотоса. Способность листьев цветка лотоса сохранять чистоту в относительно грязных местностях и самоочищаться во время дождей направила к развитию новых материалов и модификации структуры поверхности. Поверхность с таким умным покрытием может иметь экономический потенциал в случае использования на небоскрёбах, высотных зданиях и т.д. Два главных критерия поверхности для обладания гидрофобности — это шероховатость поверхности и низкая поверхностная энергия покрывающего материала. В этом исследовании супергидрофобные самоочищающиеся покрытия были получены простым, легким и дешевым методом с использованием легкодоступных материалов, таких как полидиметилсилоксан (ПДМС) и наночастицы TiO_2 , и полностью охарактеризованы для прямого применения. ПДМС представляет собой связующий слой, а наночастицы TiO_2 — армированный композит для формирования шероховатости, проявляющей супергидрофобность. Характеристика показала, что свежеприготовленное супергидрофобное покрытие имеет угол смачивания водой до $165,5^\circ$ при угле скольжения менее 5° . Также были изучены самоочищающиеся и поверхностные микрожидкостные свойства. Супергидрофобные свойства этих покрытий не меняются даже после воздействия на их поверхность низких температур и УФ-излучения. Изображения СЭМ подтверждают шероховатую структуру полученной поверхности на стекле и песчинках.

Ключевые слова: супергидрофобное покрытие, супергидрофобный песок, полидиметилсилоксан, наночастицы оксида титана, краевой угол, УФ-излучение, фасильный метод, электрокинетический потенциал.

Information about authors*

Toktarbaiuly, Olzat (*corresponding author*) — PhD in Physical Sciences, Researcher, National Laboratory Astana, Nazarbayev University, Kabanbay batyr avenue, 53, 010000, Nur-Sultan, Kazakhstan; e-mail: olzat.toktarbaiuly@nu.edu.kz; <https://orcid.org/0000-0003-4594-3435>;

Kurbanova, Aliya — Master of Chemical Sciences, Junior Researcher, National Laboratory Astana, Nazarbayev University, Kabanbay batyr avenue, 53, 010000, Nur-Sultan, Kazakhstan; e-mail: aliya.kurbanova@nu.edu.kz; Scopus ID 57208865374; <https://orcid.org/0000-0002-1261-4582>;

Ualibek, Oral — PhD in Physical Sciences, Researcher, National Laboratory Astana, Nazarbayev University, Kabanbay batyr avenue, 53, 010000, Nur-Sultan, Kazakhstan; e-mail: oral.ualibek@nu.edu.kz; Scopus ID 57116439500; <https://orcid.org/0000-0002-8482-3623>;

Seralin, Aidar — PhD in Pharmaceutical Sciences, Junior Researcher, National Laboratory Astana, Nazarbayev University, Kabanbay batyr avenue, 53, 010000, Nur-Sultan, Kazakhstan; e-mail: aidar.seralin@nu.edu.kz; <https://orcid.org/0000-0001-6001-5755>;

Zhunossova, Tomiris — Master of Physical Sciences, Consultant, National Laboratory Astana, Nazarbayev University, Kabanbay batyr avenue, 53, 010000, Nur-Sultan, Kazakhstan; e-mail: zhunossovatomiris1@gmail.com; <https://orcid.org/0000-0002-4189-1618>;

Sugurbekova, Gulnar — Doctor of Chemical Sciences, Leading Researcher, LLP “EcoStandart.kz”, Technopark of Nazarbayev University, Kabanbay batyr avenue, 53, 010000, Nur-Sultan, Kazakhstan; e-mail: sugurbekova.g.55@gmail.com; <https://orcid.org/0000-0002-6894-7247>;

Nuraje, Nurxat — Doctor of Chemical Sciences, Associate Professor, National Laboratory Astana, Nazarbayev University, Kabanbay batyr avenue, 53, 010000, Nur-Sultan, Kazakhstan; e-mail: nurxat.nuraje@nu.edu.kz; <https://orcid.org/0000-0003-4751-2719>

*The author's name is presented in the order: *Last Name, First and Middle Names*